

# Joint Transmit Signal and Beamforming Design for Integrated Sensing and Power Transfer Systems

Kenneth MacSporran Mayer, Nikita Shanin, Zhenlong You, Sebastian Lotter, Stefan Brückner, Martin Vossiek,  
Laura Cottatellucci, and Robert Schober  
Friedrich-Alexander-Universität Erlangen-Nürnberg, Germany

**Abstract**—Integrating different functionalities, conventionally implemented as dedicated systems, into a single platform allows utilising the available resources more efficiently. We consider an integrated sensing and power transfer (ISAPT) system and propose the joint optimisation of the rectangular pulse-shaped transmit signal and the beamforming vector to combine sensing and wireless power transfer (WPT) functionalities efficiently. In contrast to prior works, we adopt an accurate non-linear circuit-based energy harvesting (EH) model. We formulate and solve a non-convex optimisation problem for a general number of EH receivers to maximise a weighted sum of the average harvested powers at the EH receivers while ensuring the received echo signal reflected by a sensing target (ST) has sufficient power for estimating the range to the ST with a prescribed accuracy within the considered coverage region. The average harvested power is shown to monotonically increase with the pulse duration when the average transmit power budget is sufficiently large. We discuss the trade-off between sensing performance and power transfer for the considered ISAPT system. The proposed approach significantly outperforms a heuristic baseline scheme based on a linear EH model, which linearly combines energy beamforming with the beamsteering vector in the direction to the ST as its transmit strategy.

## I. INTRODUCTION

The growing number of Internet-of-Things (IoT) applications, ranging from smart homes to healthcare, requires the deployment of a multitude of low-power IoT devices, which future wireless networks will have to serve by facilitating communication, sensing, computation, and a supply of power [1], [2]. An efficient method for powering these low-power IoT devices through radio-frequency (RF) signals is known as wireless power transfer (WPT), which may even allow for battery-free operation of the devices [3]. In light of the tremendous number of devices, the efficient utilisation of resources, such as energy, frequency spectrum, and hardware, is indispensable. Moreover, powering the devices may require localising them first. This especially applies to the crowded sub-6 GHz band, which is occupied by different systems [4], [5]. An effective method of utilising the scarce resources more efficiently is the integration of different functionalities, such as communication, sensing, and WPT, by co-designing them into one platform, instead of employing dedicated systems for each functionality. Currently, the most prominent example of this approach is integrated sensing and communications (ISAC),

which has received significant attention and is envisioned as a key technology for next-generation wireless systems [6]. Hereby, sensing may be employed to acquire information on a target's location by considering the time delay between an emitted signal and the resulting echo signal reflected by the target [6], [7].

Unlike ISAC, the integration of sensing and power transfer (ISAPT) has received significantly less attention, despite facilitating the decongestion of spectrum and the design of hardware-efficient systems by reducing the size, cost, and power consumption. Only a few recent studies are available on ISAPT [8]–[12]. In [8], [9], the trade-off between WPT and sensing is investigated by optimising the transmit beamforming vector, whereby the authors of [9] assumed the energy harvesting (EH) receivers to be in the radiating near-field of the transmit antenna. Moreover, in [10]–[12], triple-functionality systems are considered, integrating communication, WPT, and sensing into one system by either considering all three functionalities simultaneously [10], [11], or employing ISAPT in the downlink and transmitting data in the uplink [12].

The WPT design in [8]–[12] is based on a linear EH model. Thus, these works do not capture the well-documented non-linear behaviour of practical EH circuits [3], [13]. However, accurately taking this non-linear behaviour into account, e.g., by employing the circuit-based EH model in [14], is vital when the maximisation of *harvested* power instead of *received* power is desired [3], [13]–[15]. In [8]–[12], the focus lies on optimising the beamforming design of the respective ISAPT systems while employing a transmit signal, which is favourable for one of the individual functionalities. Specifically, a continuous wave pulse signal is utilised for facilitating both sensing and WPT in [12], whereas random unit-variance signals are exploited in [8]–[11]. Although EH receivers can opportunistically harvest power from a signal designed for radar sensing, this approach may not fully exploit the ISAPT system's potential, whereas jointly co-designing the transmit signal for both functionalities can offer performance benefits. Indeed, in simultaneous wireless information and power transfer systems the optimal transmit signal represents a trade-off between the signals optimal for both communication and WPT [14]. For example, while the random Gaussian transmit signal employed in [8]–[11] is optimal for communication, it is highly suboptimal for WPT [14]. Moreover, the utilisation of random transmit signals for WPT and sensing prevents the prediction of the harvested power and the sensing

This work was (partly) funded by the Deutsche Forschungsgemeinschaft (DFG, German Research Foundation) – SFB 1483 – Project-ID 442419336, EmpkinS.

performance in a given time slot, respectively. In fact, for WPT, the transmission of rectangular pulse-shaped signals is typically assumed [14], [15]. Moreover, the optimal transmit strategy for WPT has been investigated in [14], [15], where on-off signaling was found to be optimal for single-user WPT systems. This signaling strategy is inherently similar to a pulse time-delay radar transmitting a rectangular pulse during the on-period and subsequently awaiting the reception of the echo signal reflected by the target during the off-period [7]. Therefore, in this paper, we propose to leverage this similarity to facilitate the efficient integration of WPT and sensing.

In this paper, we consider an ISAPT system comprising a multi-antenna transceiver (TRX), a single ST, and multiple EH receivers. The considered system employs a round-trip time-of-flight pulse time-delay radar for sensing. While the majority of the existing works focus on determining the angular direction of the ST with respect to the TRX [8]–[11], the proposed ISAPT system is designed to ensure the range to the ST in a certain direction is estimated with a desired accuracy by considering the time delay between the emitted transmit signal and the received echo signal. Our goal is the joint optimisation of the transmit signal and the transmit beamforming vector for ISAPT systems for integrating the sensing and WPT functionalities. To this end, we formulate an optimisation problem to maximise the weighted sum of the average harvested powers at the EH receivers while ensuring a desired sensing performance and optimise the amplitude and duration of the rectangular transmit pulse in conjunction with the transmit beamforming vector. In contrast to [8]–[12], we adopt the non-linear circuit-based EH model derived in [14], which more accurately characterises the power harvested in practical EH circuits compared to linear EH models [3], [13]. We characterise the sensing performance by ensuring the minimum power of the echo signals received from the ST is sufficient for estimation of the range to the ST with a desired accuracy within the considered coverage region. Guaranteeing a particular accuracy for estimation of the range to the ST and the adopted non-linear EH model are key differences to existing works. Prior to the solution of the proposed non-convex optimisation problem, the feasibility region of the pulse duration is determined analytically. We then propose a solution based on semidefinite relaxation (SDR) and successive convex approximation (SCA). The pulse duration yielding the largest amount of average harvested power at the EH receivers is determined through a grid search. Moreover, we discuss the trade-off between sensing performance and WPT and show that the proposed solution significantly outperforms a heuristic baseline scheme, which is based on a combination of the optimal radar and the optimal WPT transmit signals when assuming a linear EH model. Hence, the results presented in this paper deliver novel insights for the efficient integration of sensing and WPT functionalities into one common platform.

## II. SYSTEM MODEL

In this paper, we consider an ISAPT system that comprises a TRX employing a uniform linear array (ULA) equipped with

$N_t \geq 1$  antennas,  $M \geq 1$  single-antenna EH receivers, and a single ST. In Section II-A, the transmit signal model is discussed and the ISAPT system's WPT and sensing functionalities are presented in Section II-B and Section II-C, respectively.

### A. Transmit Signal Model

The TRX emits a pulse-modulated RF signal with the following equivalent complex baseband (ECB) representation

$$\mathbf{x}(t) = \sum_{k'=-\infty}^{\infty} \mathbf{x}[k']\psi(t - k'T; \tau[k']) = \mathbf{x}[k]\psi(t - kT; \tau[k]), \quad (1)$$

where  $k = \max \{y \in \mathbb{Z} | y \leq t/T\}$  with  $\mathbb{Z}$  denoting the set of integers,  $\mathbf{x}[k] \in \mathbb{C}^{N_t \times 1}$  is the transmit signal vector in the  $k$ -th time slot, and  $\psi(t; \tau[k])$  represents a rectangular pulse with magnitude 1 and duration  $\tau[k]$ , i.e.,  $\psi(t; \tau[k]) = 1$  if  $0 \leq t \leq \tau[k]$ , and zero otherwise. Furthermore, the duration of a time slot is denoted by  $T > \tau[k]$ . We note that pulse-modulated signals as in (1) are commonly utilised for the design of WPT systems [14], [15] and pulse radar systems [7]. Leveraging this similarity offers a seamless integration of WPT and sensing functionalities, and thus, we exploit the pulse time-delay radar concept in the proposed ISAPT system. We set,  $\mathbf{x}[k] = A[k]\mathbf{w}[k]$ , where  $A[k] \in \mathbb{R}$  is the signal amplitude and  $\mathbf{w}[k] \in \mathbb{C}^{N_t \times 1}$  is the beamforming vector. The energy of  $\mathbf{w}[k]$  is normalised to unity, i.e.,  $\|\mathbf{w}[k]\|_2^2 = 1$ , where  $\|\cdot\|_2$  is the Euclidean norm. Thus,  $\tau[k]$ ,  $A[k]$ , and  $\mathbf{w}[k]$  represent the optimisation variables for jointly optimising the duration, amplitude, and beamforming of the transmit signal, respectively. The dependence of  $\tau[k]$ ,  $A[k]$ , and  $\mathbf{w}[k]$  on symbol interval  $k$  is dropped in the notation in the remainder of this paper for better legibility.

### B. Wireless Power Transfer System

We assume a fading channel  $\mathbf{h}_m \in \mathbb{C}^{N_t \times 1}$  between the TRX and EH node  $m$  with  $m = 1, \dots, M$ . Moreover, perfect knowledge of the channel vectors  $\mathbf{h}_m$ ,  $\forall m = 1, \dots, M$ , is assumed at the TRX. Consequently, the instantaneous power of the received signal at the  $m$ -th EH receiver in interval  $[kT, kT + \tau]$  is given by

$$P_m = P_m(A\mathbf{w}) = A^2 |\mathbf{h}_m^H \mathbf{w}|^2. \quad (2)$$

For WPT, we neglect the impact of additive noise due to its negligible contribution to the average harvested power [15].

Each EH receiver is equipped with a rectenna comprising an antenna, a matching circuit, a non-linear rectifier, such as a Schottky diode combined with a low-pass filter, and a load resistor [14], [15]. We adopt the non-linear circuit-based EH model proposed in [14], which was derived by accurately analysing the current flow through the electrical EH circuit [14]. The harvested power  $\tilde{\varphi}(P_m)$  from the pulse at the  $m$ -th EH receiver in time slot  $k$  is given by  $\tilde{\varphi}(P_m) = \min \{\varphi(P_m), \varphi(P_{\max})\}$ , which is bounded due to the saturation of practical EH circuits caused by the breakdown of the employed Schottky diodes at high received powers

[14]. Hereby, the non-linear monotonically increasing function  $\varphi(P_m)$  models the EH circuit and is given by [14], [15]

$$\varphi(P_m) = \left[ \frac{1}{a} W_0 \left( a e^a I_0 \left( C \sqrt{2P_m} \right) \right) - 1 \right]^2 I_s^2 R_L, \quad (3)$$

where  $W_0(\cdot)$  and  $I_0(\cdot)$  are the principal branch of the Lambert-W function and the zeroth order modified Bessel function of the first kind, respectively. The parameters  $a$  and  $C$  depend on the employed EH circuit and are independent of the received signal [14], [15]. Note that operating Schottky diodes in the breakdown regime should be avoided [16, Remark 5]. Therefore, we enforce  $P_m \leq P_{\max}$  and consequently,  $\tilde{\varphi}(P_m) = \varphi(P_m)$ . The average harvested power at the  $m$ -th EH node in time slot  $k$  is determined by averaging the power received during pulse duration  $\tau$  over time slot  $T$ . We consider the weighted sum of average harvested powers among all EH receivers during time slot  $k$ , which is given by

$$\phi(A\mathbf{w}, \tau) = \frac{\tau}{T} \sum_{m=1}^M \beta_m \varphi(P_m), \quad (4)$$

where  $\beta_m \in [0, 1]$ ,  $\forall m = 1, \dots, M$ , is the weight associated with the  $m$ -th EH receiver such that  $\sum_m \beta_m = 1$ . The  $\beta_m$ ,  $\forall m = 1, \dots, M$ , can be chosen to, e.g., ensure EH fairness among the EH nodes.

### C. Sensing System

We define the location of an ST by the tuple  $(R, \alpha)$ , whereby  $R$  is the range from the TRX to the ST and  $\alpha$  is the angular direction of the ST. The objective of the proposed ISAPT system is to ensure the range  $R$  to the ST at angular direction  $\alpha$  can be estimated to a desired accuracy. Specifically, angular direction  $\alpha$  is probed within a certain time frame  $T_{\text{sen}}$ , whereby a meaningful echo signal is only received if a ST is present in direction  $\alpha$ . The absence of a meaningful echo signal implies no ST is present at  $\alpha$  and thus, a different angular direction  $\alpha'$  is explored. Here, we focus on the case when a meaningful echo signal is detected from angular direction  $\alpha$ . The duration of time frame  $T_{\text{sen}}$  is assumed fixed and determined by the characteristics of the TRX and upper-bounded by the coherence time  $T_{\text{coh}}$  of the fading channels between the TRX and the EH receivers, i.e.,  $T \leq T_{\text{sen}} \leq T_{\text{coh}}$ . In this paper, we assume  $T_{\text{coh}}$  and  $T_{\text{sen}}$  are on the order of milliseconds, whereas time slot duration  $T$  is typically on the order microseconds to nanoseconds [7], i.e.,  $T_{\text{sen}} \gg T$ . The location of the ST is assumed to be quasi-static, i.e., the ST remains approximately static during  $T_{\text{sen}}$ . During  $T_{\text{sen}}$ , the ISAPT system uses pulses from multiple time slots, each of duration  $T$ , to perform coherent pulse integration, which is discussed in detail in Section II-C2.

Next, we establish the relationship between the coverage range, within which an estimation of the range  $R$  is desired, the pulse duration  $\tau$ , and the time slot duration  $T$ .

1) *Bounds on  $\tau$  and  $T$* : While transmitting, the TRX cannot receive a reflected echo signal, which is necessary for localising the ST [7]. Therefore, an upper bound on pulse

duration  $\tau$  is necessary. This is determined by the minimum range  $R_{\min}$  the ST may be located at [7], i.e.,

$$\tau \leq \tau_{\max} = \frac{2 R_{\min}}{c}, \quad (5)$$

where  $c$  is the speed of light. The duration of a time slot  $T$  is constrained by the maximum coverage range  $R_{\max}$ . Specifically, the shortest possible time slot duration  $T_{\min}$  to ensure a target is reached anywhere within the coverage region and the echo signal is received back when employing a very short rectangular pulse, i.e.,  $\tau \rightarrow 0$ , is  $T \geq T_{\min} = (2 R_{\max})/c$  [7]. Moreover, since  $R_{\min} \leq R \leq R_{\max}$ , time slot duration  $T$  can be set as follows

$$T(\tau) = T_{\min} + \tau = \frac{2 R_{\max}}{c} + \tau, \quad (6)$$

where  $T(\tau)$  exceeds the minimum required time  $T_{\min}$  by the pulse duration  $\tau$ , which is yet to be optimised for ISAPT, such that the full echo signal is received before the next pulse is transmitted.

Next, we characterise the accuracy of estimating the range  $R$  to guarantee the desired sensing performance within the coverage region  $R_{\min} \leq R \leq R_{\max}$ .

2) *Sensing accuracy*: By ensuring that the minimum echo signal power  $P_{\text{ST}}$ , i.e., the power of the echo received from the ST at  $R_{\max}$ , is sufficient for attaining a particular accuracy of estimating the range, the desired accuracy is guaranteed to be attained in the full coverage region, i.e.,  $R \leq R_{\max}$ . The minimum echo signal power  $P_{\text{ST}}$  during a time slot follows from the radar equation and is given by [7]

$$\frac{\tau}{T(\tau)} P_{\text{ST}} = \frac{\tau A^2}{T(\tau)} |\mathbf{u}^H \mathbf{w}|^2 \underbrace{\frac{\lambda^2 \sigma_{\text{RCS}}}{(4\pi)^3 R_{\max}^4}}_{=z_1} \|\mathbf{u}\|_2^2, \quad (7)$$

where  $\mathbf{u} = [1, e^q, e^{2q}, \dots, e^{(N_t-1)q}]^T \in \mathbb{C}^{N_t \times 1}$  with  $q = -j\pi \sin(\alpha) \Delta_{\text{TRX}}$  denotes the vector of phase delays in direction  $\alpha$ ,  $\Delta_{\text{TRX}}$  is the transmit antenna spacing,  $\lambda$  is the wavelength, and  $\sigma_{\text{RCS}}$  is the radar cross-section (RCS) of the ST. The receive beamformer is chosen according to direction  $\alpha$  for maximising the signal power at the detector.

The received echo at the TRX<sup>1</sup> is impaired by additive white Gaussian noise (AWGN) with noise power  $\sigma_n^2$ . In this paper, we consider range estimation based on the estimated time delay  $T_R$  between the emission of the transmit signal and the reception of the echo signal [7]. Hence, the sensing performance of the ISAPT system is characterised by the accuracy with which the system is capable of determining time delay  $T_R$  [7]. Since the estimated range is a linear function of  $T_R$ , the estimation error of the range,  $\hat{R}$ , defined as the root mean squared (RMS) error between the estimated range and the true range, is given by  $\hat{R} = (\hat{T}_R c/2)$ , where  $\hat{T}_R$  is the RMS error of the estimated time delay  $T_R$  [7].

<sup>1</sup>The study of additional disturbing influences, such as additional system and propagation losses, on the minimum echo signal power and thus, the system performance, is an interesting topic for future work. Here, we aim at determining the maximum achievable system performance, and therefore, we neglect these additional influences.

Hereby, the accuracy of estimating the time delay is limited by noise. Thus, a large signal-to-noise ratio (SNR) is required to obtain an accurate estimate of  $T_R$  and thus, typically, the echoes of multiple pulses are exploited for the estimation of  $T_R$  [7]. To this end, the proposed ISAPT system employs coherent pulse integration. Consequently, the total signal power at the TRX in time frame  $T_{\text{sen}}$  grows linearly with the number of pulses per  $T_{\text{sen}}$ . For maximum performance,  $N(\tau) = \max \{y \in \mathbb{Z} | y \leq T_{\text{sen}}/T(\tau)\}$  pulses are employed for estimating  $T_R$  since the echo signals received in different time slots are added coherently, whereas the noise in different time slots is assumed to be uncorrelated [7]. In the following, we assume  $N(\tau) = T_{\text{sen}}/T(\tau)$  for analytical tractability. Moreover, the impact of multipath components is neglected since they arrive after the line-of-sight (LoS) echo signal. As a result, for the considered rectangular pulse shape,  $\hat{T}_R$  is given by [7]

$$\hat{T}_R = \frac{1}{B} \sqrt{\underbrace{\frac{\sigma_n^2}{4 T_{\text{sen}}}}_{=z_2} \frac{[T(\tau)]^2}{\tau P_{\text{ST}}}}, \quad (8)$$

where  $B$  is the bandwidth available to the ISAPT system.

### III. PROBLEM FORMULATION AND PROPOSED SOLUTION

#### A. Problem Formulation

The objective is to maximise the weighted sum of the average harvested powers at the EH receivers (4) while ensuring the desired accuracy of estimating the range  $R$  by limiting the RMS error  $\hat{R}$  to lie below a certain threshold  $\hat{R}_{\text{max}}$ , which defines the maximum tolerated sensing error. To this end, we jointly optimise the transmit beamforming and the duration and amplitude of the rectangular transmit pulse in symbol interval  $k$ . Mathematically, this is formulated as the following optimisation problem

$$\underset{\tau, A, \mathbf{w}}{\text{maximise}} \quad \phi(A\mathbf{w}, \tau) \quad (9a)$$

$$\text{subject to} \quad \text{C1: } z \sqrt{\frac{[T(\tau)]^2}{\tau A^2 \|\mathbf{u}^H \mathbf{w}\|^2}} \leq \hat{R}_{\text{max}}, \quad (9b)$$

$$\text{C2: } \frac{\tau}{T(\tau)} A^2 \|\mathbf{w}\|_2^2 \leq P_{\text{avg}}, \quad (9c)$$

$$\text{C3: } A^2 \|\mathbf{w}\|_2^2 \leq P_p, \quad (9d)$$

$$\text{C4: } A^2 |\mathbf{h}_m^H \mathbf{w}|^2 \leq P_{\text{max}}, \forall m = 1 \dots M, \quad (9e)$$

$$\text{C5: } 0 \leq \tau \leq \tau_{\text{max}} \quad (9f)$$

where  $z = (c\sqrt{z_2})/(2B\sqrt{z_1})$  with  $z_1$  and  $z_2$  defined in (7) and (8), respectively. Moreover, we impose constraints on the average transmit power  $P_{\text{avg}}$  and the peak transmit power  $P_p$  in (9c) and (9d), respectively. Note that (9e) avoids the EH receivers operating in the breakdown regime by limiting the peak received power to  $P_{\text{max}}$ . Problem (9) is non-convex due to the objective function (9a) and constraints C1, C2, C3, and C4.

#### B. Feasibility Region of Problem (9)

Prior to solving Problem (9), we determine the feasibility region  $\mathcal{T}$  of  $\tau$  analytically by taking into account the constraint on the sensing accuracy C1 and the upper bound imposed in C5.

**Proposition 1.** *The pulse duration  $\tau$  has the feasible region  $\mathcal{T} = [\tau_{\min}, \tau_{\max}]$ , where the minimum pulse duration  $\tau_{\min}$  is given by*

$$\tau_{\min} = \frac{1}{2} \left( z_3 - z_4 - \sqrt{z_3^2 - 2z_3 z_4} \right), \quad (10)$$

with  $z_3 = P_p \|\mathbf{u}\|_2^2 \hat{R}_{\text{max}}^2 / z^2 > 0$  and  $z_4 = 4R_{\text{max}}/c > 0$ .

*Proof.* The proof is provided in Appendix A.  $\square$

*Remark:* Note that the pulse duration  $\tau \in \mathcal{T}$  impacts the feasibility region of  $A$  and  $\mathbf{w}$  as these optimisation variables are coupled in Problem (9). The non-trivial relationship of the optimisation variables is investigated in Section IV.

#### C. Problem Reformulation and Proposed Solution

Obtaining a solution to Problem (9) is challenging due to the non-convexity of the problem and the coupling of optimisation variables  $\tau$  and  $A$ . Our proposed approach for solving Problem (9) is based on a one-dimensional grid search over  $\tau$  and the application of SDR and SCA at every point of the grid. To perform a one-dimensional grid search over  $\tau$ , the interval  $\mathcal{T}$  is discretised into a set of  $n_\tau$  equally-spaced values and we denote this set by  $\mathcal{T}_{n_\tau}$ .

First, we decouple optimisation variables  $A$  and  $\mathbf{w}$  from  $\tau$  and solve Problem (9) for  $A_\tau$  and  $\mathbf{w}_\tau$  at every point on the grid, i.e.,  $\tau \in \mathcal{T}_{n_\tau}$ . In the following, we propose an approach for obtaining the solution  $A_\tau^*$  and  $\mathbf{w}_\tau^*$ , which maximises the objective function (9a), for a given pulse duration  $\tau \in \mathcal{T}_{n_\tau}$ . To this end, we apply the change of variables  $\mathbf{v} = A_\tau \mathbf{w}_\tau$ . Next, we define matrix variable  $\mathbf{V} = \mathbf{v}\mathbf{v}^H$  which, by construction, is Hermitian and has a rank of 1, i.e.,  $\text{rank}(\mathbf{V}) = 1$ . Note that  $\mathbf{V}$  is a positive semi-definite (PSD) matrix, i.e.,  $\mathbf{V} \succeq \mathbf{O}$ , where  $\mathbf{O} \in \mathbb{R}^{N_t \times N_t}$  denotes the all-zero matrix. This yields the following equivalent reformulation of Problem (9) for a fixed value of  $\tau \in \mathcal{T}_{n_\tau}$

$$\underset{\mathbf{V} \succeq \mathbf{O}}{\text{maximise}} \quad \Phi(\mathbf{V}) \quad (11a)$$

$$\text{subject to} \quad \widehat{\text{C1}}: \varepsilon_1(\tau) \leq \text{Tr}\{\mathbf{U}\mathbf{V}\}, \quad (11b)$$

$$\widehat{\text{C2/3}}: \text{Tr}\{\mathbf{V}\} \leq \varepsilon_2(\tau), \quad (11c)$$

$$\widehat{\text{C4}}: \text{Tr}\{\mathbf{H}_m \mathbf{V}\} \leq P_{\text{max}}, \forall m = 1 \dots M, \quad (11d)$$

$$\widehat{\text{C6}}: \text{rank}(\mathbf{V}) = 1, \quad (11e)$$

where  $\Phi(\mathbf{V}) = (\tau/T(\tau)) \sum_{m=1}^M \varphi(\text{Tr}\{\mathbf{H}_m \mathbf{V}\})$  with  $\mathbf{H}_m = \mathbf{h}_m \mathbf{h}_m^H$ ,  $\forall m = 1 \dots M$ ,  $\mathbf{U} = \mathbf{u}\mathbf{u}^H$ ,  $\varepsilon_1(\tau) = (z^2 [T(\tau)]^2) / (\tau \hat{R}_{\text{max}}^2) > 0$ , and  $\varepsilon_2(\tau) = \min\{(T(\tau)/\tau) P_{\text{avg}}, P_p\} > 0$ . Note that Problem (11) is non-convex due to the objective function (11a) and  $\widehat{\text{C6}}$ . We propose the application of SCA to solve Problem (11) [17].

Furthermore,  $\widehat{C6}$  is dropped. In Proposition 2, we will show that the solution in every iteration of the SCA algorithm satisfies  $\widehat{C6}$  implicitly. In iteration  $i \geq 0$  of the SCA algorithm, we construct the following lower bound of the objective function

$$\Phi(\mathbf{V}) \geq \hat{\Phi}(\mathbf{V}, \mathbf{V}^i), \quad (12)$$

with

$$\hat{\Phi}(\mathbf{V}, \mathbf{V}^i) = \Phi(\mathbf{V}^i) + \frac{\tau}{T(\tau)} \left( \sum_{m=1}^M \varphi'(\text{Tr}\{\mathbf{H}_m \mathbf{V}^i\}) \text{Tr}\{\mathbf{H}_m \mathbf{V} - \mathbf{H}_m \mathbf{V}^i\} \right). \quad (13)$$

Here,  $\varphi'(\cdot)$  denotes the derivative of  $\varphi(\cdot)$  with respect to the input power evaluated at  $\text{Tr}\{\mathbf{H}_m \mathbf{V}^i\}$  and  $\mathbf{V}^i$  is the solution obtained in the  $i$ -th iteration of the algorithm. We utilise  $\mathbf{V}^0 = (P_p / \|\mathbf{u}\|_2^2) (\mathbf{u}\mathbf{u}^H)$  as a feasible initialisation of the algorithm to satisfy the desired sensing accuracy. Consequently, the optimisation problem solved in every iteration  $i$  of the algorithm is given by

$$\mathbf{V}^{i+1} = \underset{\mathbf{V} \succeq 0}{\text{argmax}} \hat{\Phi}(\mathbf{V}, \mathbf{V}^i) \quad \text{subject to} \quad \widehat{C1}, \widehat{C2/3}, \widehat{C4}, \quad (14)$$

which is a convex optimisation problem that can be solved efficiently with, for example, CVXPY [18]. Next, we show that the solution of Problem (14) yields a rank-one matrix.

**Proposition 2.** *In each iteration  $i \geq 0$ , the solution  $\mathbf{V}^{i+1}$  of Problem (14) satisfies  $\text{rank}(\mathbf{V}^{i+1}) = 1$ .*

*Proof.* The proof is provided in Appendix B.  $\square$

The beamforming vector  $\mathbf{w}_\tau^*$  and the signal amplitude  $A_\tau^*$  are obtained as the dominant normalised eigenvector and the square root of the corresponding eigenvalue of the rank-one matrix  $\mathbf{V}^i$  obtained in the final iteration of the algorithm, respectively. The proposed algorithm is summarised in Algorithm 1. Note that the proposed algorithm converges to a stationary point of (9) for  $\mathcal{T}_{n_\tau}$  [19]. The computational complexity of a single iteration of the algorithm is  $\mathcal{O}(MN_t^{3.5} + M^2N_t^{2.5} + M^3N_t^{0.5})$ , where  $\mathcal{O}(\cdot)$  denotes the big-O notation [15]. Lastly, the optimal pulse duration is found by evaluating  $\tau^* = \underset{\tau}{\text{argmax}} \phi(A_\tau^* \mathbf{w}_\tau^*, \tau)$ .

---

**Algorithm 1** Procedure for obtaining  $\tau^*, A^*, \mathbf{w}^*$

---

**Initialise:**  $\mathbf{V}^0 = \frac{P_p}{\|\mathbf{u}\|_2^2} (\mathbf{u}\mathbf{u}^H)$ ,  $i = 0$ ,  $h^0 = 0$ ,  $h^{-1} = 2\epsilon_{\text{SCA}}$  with  $\epsilon_{\text{SCA}}$  denoting the tolerance.

**for**  $\tau \in \mathcal{T}_{n_\tau}$  **do**

**while**  $|h^i - h^{i-1}| > \epsilon_{\text{SCA}}$  **do**

        Obtain  $\mathbf{V}^{i+1}$  by solving (14) for  $\mathbf{V}^i$

        Determine  $h^{i+1} = \Phi(\mathbf{V}^{i+1})$  and set  $i = i + 1$

**end while**

$\mathbf{w}_\tau^*$  is the dominant normalised eigenvector of  $\mathbf{V}^i$ .

$A_\tau^*$  is the square root of the eigenvalue associated with  $\mathbf{w}_\tau^*$ .

**end for**

Determine  $\tau^* = \underset{\tau}{\text{argmax}} \phi(A_\tau^* \mathbf{w}_\tau^*, \tau)$

**Output:**  $\tau^*, A^* = A_{\tau^*}^*, \mathbf{w}^* = \mathbf{w}_{\tau^*}^*$

---

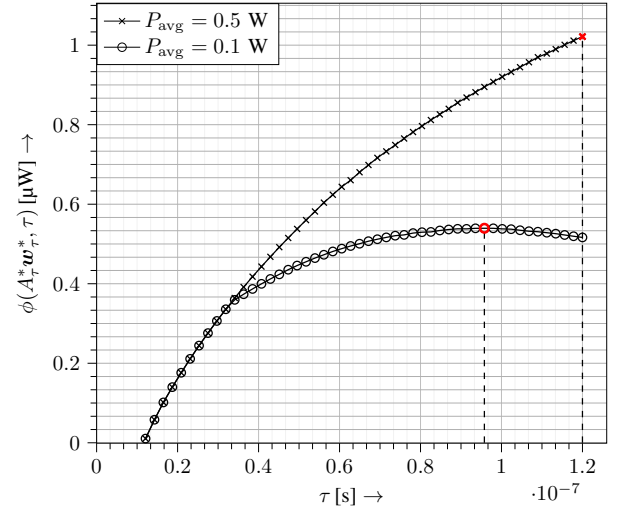


Fig. 1: Average harvested power  $\phi(A_\tau^* \mathbf{w}_\tau^*, \tau)$  for  $\tau \in \mathcal{T}_{n_\tau}$ . The optimal pulse duration  $\tau^*$  is highlighted in red.

#### IV. RESULTS AND PERFORMANCE EVALUATION

In the following, we consider an ISAPT system with  $M = 3$  EH nodes with weights  $\beta_m = 1/M$ ,  $\forall m = 1, \dots, M$ , which are located at a distance of 5 m from the TRX at  $45^\circ$ ,  $60^\circ$ , and  $75^\circ$ , respectively. The channel  $\mathbf{h}_m$ ,  $\forall m = 1, \dots, M$ , between the TRX and EH node  $m$  is modelled as a Rician fading channel. Thereby, we calculate the respective path loss as  $\lambda^2 / (4\pi R_m)^2$ , where  $R_m$  is the distance to the  $m$ -th EH node, and assume Rician K-factor  $\kappa = 1$ . Moreover, the ST is located at  $\alpha = -60^\circ$ . We assume  $\sigma_{\text{RCS}} = 1 \text{ m}^2$ , which is a typical value for several applications and, e.g., approximately the RCS of a human that may be equipped with a wearable device [7]. Table I provides all relevant simulation parameters. All results are averaged over 100 EH channel realisations.

TABLE I: Simulation parameters.

General parameters	WPT parameters	Sensing parameters
$P_{\text{avg}} \in \{0.1, 0.5\} \text{ W}$	$a = 1.29$	$B = 10 \text{ MHz}$
$P_p \in \{0.5, 1\} \text{ W}$	$C = 1.55 \cdot 10^3$	$\sigma_n^2 = -80 \text{ dBm}$
$\lambda = 0.125 \text{ m}$	$I_s = 5 \text{ }\mu\text{A}$	$R_{\text{max}} = 20 \text{ m}$
Channel realisations: 100	$R_L = 10 \text{ k}\Omega$	$R_{\text{min}} \in \{3, 5, 18\} \text{ m}$
$N_t = 10$	$P_{\text{max}} = 25 \text{ }\mu\text{W}$	$\hat{R}_{\text{max}} \in [0.01, 0.06] \text{ m}$
$\epsilon_{\text{SCA}} = 1 \cdot 10^{-7}$	$M = 3$	$\sigma_{\text{RCS}} = 1 \text{ m}^2$
$n_\tau = 50$	Rician K-factor: 1	$T_{\text{sen}} = 1 \text{ ms}$
$\Delta_{\text{TRX}} = \lambda/2$	$T_{\text{coh}} = 1 \text{ ms}$	

##### A. Optimal Pulse Duration

First, we investigate the average amount of harvested power (4) for all  $\tau \in \mathcal{T}_{n_\tau}$ , i.e., from the smallest to the largest value of  $\mathcal{T}$ , thereby determining the optimal pulse duration  $\tau^*$ . To this end, we set  $\hat{R}_{\text{max}} = 0.02 \text{ m}$ ,  $R_{\text{min}} = 18 \text{ m}$ , and  $P_p = 0.5 \text{ W}$  and investigate the average amount of harvested power (4) versus  $\tau \in \mathcal{T}_{n_\tau}$  for  $P_{\text{avg}} = 0.1 \text{ W}$  and  $P_{\text{avg}} = 0.5 \text{ W}$ , respectively, in Fig. 1. Next, the non-trivial relationship among the optimisation variables is studied. When  $P_{\text{avg}}$  is large, i.e.,  $P_{\text{avg}} = 0.5 \text{ W}$ , the average harvested power increases with  $\tau \in \mathcal{T}_{n_\tau}$ , and thus,  $\tau^* = \tau_{\text{max}} = 1.2 \cdot 10^{-7} \text{ s}$ , which is highlighted by the red cross in Fig. 1. Note that  $\tau^*/T(\tau^*) \approx 47\%$ . In fact, constraint C2 is not tight in this case and the solution of

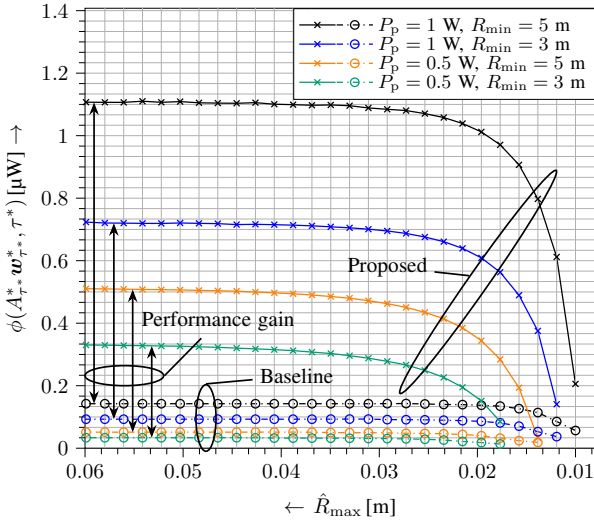


Fig. 2: Average harvested power  $\phi(A_{\tau^*}^* \mathbf{w}_{\tau^*}^*, \tau^*)$  vs.  $\hat{R}_{\max}$ . Solid lines with crosses correspond to the proposed solution, while dash-dotted lines with circles indicate the baseline scheme.

Problem (9) is determined by the sensing accuracy constraint C1. However, this behaviour does not apply for low  $P_{\text{avg}}$ , i.e.,  $P_{\text{avg}} = 0.1 \text{ W}$ , as, in this case, constraint C2 becomes increasingly important. Then, as  $\tau$  grows, we first observe an increase of the harvested power up to  $\tau^* \approx 0.96 \cdot 10^{-7} \text{ s}$ , which is highlighted by the red circle in Fig. 1, followed by a decrease of harvested power. In this case,  $\tau^*/T(\tau^*) \approx 38\%$ . Consequently, determining the optimal pulse duration  $\tau^*$  of the ISAPT system is important to maximise the harvested power at the EH nodes.

### B. Performance Evaluation and Trade-Off Between Sensing Accuracy and Harvested Power

Next, the trade-off between sensing performance and WPT is investigated. We compare the performance of our proposed solution to a baseline scheme, which linearly combines the optimal transmit signal strategy for WPT when assuming a linear EH model, i.e., energy beamforming [20], with the optimal radar sensing signal, i.e., the beamsteering vector towards the ST. The weighting factor for the linear combination of the two signals is set to satisfy constraint C1 with equality, such that only the minimum required sensing accuracy is achieved and the remaining transmit power is dedicated to WPT. We utilise the optimal pulse duration for the proposed scheme and the baseline scheme, which are both obtained through the grid search over  $\tau$ .

For the results in Fig. 2, we set  $P_{\text{avg}} = 0.5 \text{ W}$  and investigate the trade-off between the average harvested power (4) and the sensing accuracy  $\hat{R}_{\max}$  for different  $R_{\min}$  and  $P_p$ . We observe from Fig. 2 that the proposed solution (solid lines with crosses) outperforms the baseline scheme (dash-dotted lines with circles) by a considerable margin indicated by the arrows in Fig. 2. For larger  $P_p$ , the ISAPT system can achieve higher sensing accuracy and average harvested power. The same observation is made for larger  $R_{\min}$  since a longer pulse duration  $\tau$  is admissible for larger  $R_{\min}$ , which follows

from (5). Furthermore, we observe a trade-off between average harvested power (4) and sensing accuracy. In fact, for a smaller tolerated maximum range estimation error  $\hat{R}_{\max}$ , more power has to be transmitted towards the ST to attain a stronger echo signal, and thus, the average harvested power decreases. Thus, the joint optimisation of the transmit signal and beamforming design taking into account the non-linearity of EH circuits, is essential for efficient ISAPT.

## V. CONCLUSION

In this paper, we jointly optimised the transmit rectangular pulse and the beamforming vector for an ISAPT system with multiple EH nodes and a single ST while considering a non-linear circuit-based EH model. Hereby, the objective was to maximise the total amount of harvested power in a time slot while ensuring the required sensing performance for estimating the range to the ST with a desired accuracy. We determined the feasible region of the pulse duration analytically and proposed a low-complexity solution to the non-convex problem based on a one-dimensional grid search, SDR, and SCA. Analytically, the solution at each iteration of the SCA algorithm was shown to be a rank-one matrix, thus yielding the optimal beamformer and amplitude of the transmit signal, respectively. The proposed low-complexity solution significantly outperforms a baseline scheme, the transmit strategy of which is based on a linear combination of energy beamforming and the radar beamsteering vector. This underscores the importance of accurately modelling of the non-linear EH circuit for efficient ISAPT system design. A generalisation of the problem to multiple STs or the incorporation of additional communication links present interesting topics for future work.

## APPENDIX A

A lower bound on pulse duration  $\tau$  is obtained by assuming that the tolerated accuracy level in C1 is achieved with equality and all the available power is utilised for ST localisation, i.e.,  $A = \sqrt{P_p}$  and  $\mathbf{w} = \mathbf{u}/\|\mathbf{u}\|_2$ . This leads to the following condition for the lower bound  $\tau_{\min}$

$$\frac{z^2 [T(\tau_{\min})]^2}{\tau_{\min} \hat{R}_{\max}^2} = P_p \|\mathbf{u}\|_2^2. \quad (15)$$

Rewriting (15), yields a quadratic equation for  $\tau_{\min}$  as follows

$$\tau_{\min}^2 + \tau_{\min} [z_4 - z_3] + \frac{4 R_{\max}^2}{c^2} = 0, \quad (16)$$

with  $z_3 = (P_p \|\mathbf{u}\|_2^2 \hat{R}_{\max}^2)/z^2 > 0$  and  $z_4 = (4 R_{\max})/c > 0$ , which has the following two solutions

$$\tau_{\min}^{(I),(II)} = \frac{1}{2} \left( z_3 - z_4 \pm \sqrt{z_3^2 - 2z_3z_4} \right). \quad (17)$$

The smallest feasible  $\tau_{\min}$  is given by the minimum of  $\tau_{\min}^{(I)}$  and  $\tau_{\min}^{(II)}$ , which has to be positive for any  $z_3$  and  $z_4$  to satisfy C1. In the following, we show that  $\tau_{\min} = \frac{1}{2} (z_3 - z_4 - \sqrt{z_3^2 - 2z_3z_4}) > 0$  holds. Since  $\tau_{\min}$  is real-

valued,  $z_3^2 \geq 2z_3z_4$  must hold in (17), and this in turn implies  $z_3 > z_3/2 \geq z_4 > 0$ , i.e.,  $z_3 - z_4 > 0$ . Moreover,

$$z_3 - z_4 > \sqrt{z_3^2 - 2z_3z_4} \iff z_3^2 - 2z_3z_4 + z_4^2 > z_3^2 - 2z_3z_4, \quad (18)$$

holds by definition since  $z_4 > 0$ , which concludes the proof.

#### APPENDIX B

The gap between Problem (14) and its dual problem is equal to zero since strong duality holds [21]. The Lagrangian of Problem (14) is given by

$$\mathcal{L} = -\hat{\Phi}(\mathbf{V}, \mathbf{V}^i) - \mu \text{Tr}\{\mathbf{U}\mathbf{V}\} + \xi \text{Tr}\{\mathbf{V}\} + \sum_{m=1}^M \mu_m \text{Tr}\{\mathbf{H}_m \mathbf{V}\} - \text{Tr}\{\mathbf{Y}\mathbf{V}\} + \gamma, \quad (19)$$

where  $\mu$ ,  $\xi$ , and  $\mu_m$ ,  $\forall m = 1, \dots, M$ , are the Lagrangian multipliers related to constraints  $\widehat{\text{C1}}$ ,  $\widehat{\text{C2/3}}$ , and  $\widehat{\text{C4}}$ , respectively. Moreover,  $\mathbf{Y}$  is the Lagrangian multiplier associated with the constraint restricting  $\mathbf{V}$  to a PSD matrix and  $\gamma$  accounts for all terms not involving  $\mathbf{V}$ . We note that the Karush-Kuhn-Tucker (KKT) conditions are satisfied for the optimal solution  $\mathbf{V}^{i+1}$  of Problem (14) and  $\check{\mu}, \check{\xi}, \check{\mu}_m$ ,  $\forall m = 1, \dots, M$ , and  $\check{\mathbf{Y}}$  are the solutions of the dual problem of Problem (14). The KKT conditions are given by

$$\nabla_{\mathbf{V}} \mathcal{L} = \mathbf{O} \quad (20a)$$

$$\check{\mu} \geq 0, \check{\xi} \geq 0, \check{\mu}_m \geq 0, \forall m = 1, \dots, M, \check{\mathbf{Y}} \succcurlyeq \mathbf{O} \quad (20b)$$

$$\check{\mathbf{Y}}\check{\mathbf{V}} = \mathbf{O}, \quad (20c)$$

where  $\nabla_{\mathbf{V}} \mathcal{L}$  is the gradient of  $\mathcal{L}$  with respect to  $\mathbf{V}$  and the matrix  $\mathbf{O} \in \mathbb{R}^{N_t \times N_t}$  denotes the all-zero matrix. From (20a), we obtain  $\check{\mathbf{Y}} = \check{\xi} \mathbf{I} - \mathbf{Z}$ , where  $\mathbf{I} \in \mathbb{R}^{N_t \times N_t}$  is the identity matrix of size  $N_t$ , and  $\mathbf{Z} = \check{\mu} \mathbf{U} - \sum_{m=1}^M (\check{\mu}_m - (\tau/T(\tau))\varphi'(\text{Tr}\{\mathbf{H}_m \mathbf{V}^i\})) \mathbf{H}_m$ . Note that by definition of  $\mathbf{U}$  and  $\mathbf{H}_m$ ,  $\forall m = 1, \dots, M$ ,  $\mathbf{Z}$  is a Hermitian matrix, i.e.,  $\mathbf{Z}^H = \mathbf{Z}$ , and thus, it can be expressed as  $\mathbf{Z} = \mathbf{P} \mathbf{\Lambda} \mathbf{P}^H$ , where the columns of unitary matrix  $\mathbf{P}$  are the eigenvectors of  $\mathbf{Z}$  and  $\mathbf{\Lambda}$  is a diagonal matrix containing the corresponding real-valued eigenvalues. Consequently,  $\check{\mathbf{Y}}$  is given by

$$\check{\mathbf{Y}} = \mathbf{P} (\check{\xi} \mathbf{I} - \mathbf{\Lambda}) \mathbf{P}^H. \quad (21)$$

Let  $\delta_{\max}$  denote the largest eigenvalue of  $\mathbf{Z}$ , which, with probability 1, has algebraic multiplicity 1 due to the randomness of the channel. If  $\check{\xi} > \delta_{\max}$ , then  $\check{\mathbf{Y}}$  is invertible and thus,  $\text{rank}(\check{\mathbf{Y}}) = N_t$ . Consequently,  $\mathbf{V}^{i+1} = \mathbf{O}$  with  $\text{rank}(\mathbf{V}^{i+1}) = 0$ , which follows from (20c). However,  $\mathbf{V}^{i+1} = \mathbf{O}$  is infeasible since it violates constraint  $\widehat{\text{C1}}$ . If  $\check{\xi} < \delta_{\max}$ , then at least one eigenvalue of  $\check{\mathbf{Y}}$  is negative, which implies that  $\check{\mathbf{Y}}$  is not a PSD matrix, thereby contradicting (20b). Consequently,  $\check{\xi} = \delta_{\max} \geq 0$  must hold, which implies  $\text{rank}(\check{\mathbf{Y}}) = N_t - 1$ . The application of Sylvester's rank inequality to (20c) yields

$$0 = \text{rank}(\check{\mathbf{Y}} \mathbf{V}^{i+1}) \geq \text{rank}(\check{\mathbf{Y}}) + \text{rank}(\mathbf{V}^{i+1}) - N_t, \quad (22)$$

which implies  $1 \geq \text{rank}(\mathbf{V}^{i+1})$ . Consequently, the optimal solution  $\mathbf{V}^{i+1}$  to Problem (14) satisfies  $\text{rank}(\mathbf{V}^{i+1}) = 1$ .

#### REFERENCES

- [1] W. Saad, M. Bennis, and M. Chen, "A Vision of 6G Wireless Systems: Applications, Trends, Technologies, and Open Research Problems," *IEEE Netw.*, vol. 34, no. 3, pp. 134–142, May 2020.
- [2] W. Tong and P. Zhu, *6G: The Next Horizon: From Connected People and Things to Connected Intelligence*. Cambridge University Press, 2021, pp. 24–26.
- [3] B. Clerckx, R. Zhang, R. Schober, D. W. K. Ng, D. I. Kim, and H. V. Poor, "Fundamentals of Wireless Information and Power Transfer: From RF Energy Harvester Models to Signal and System Designs," *IEEE J. Sel. Areas Commun.*, vol. 37, no. 1, pp. 4–33, Jan. 2019.
- [4] F. Liu, Y. Cui, C. Masouros, et al., "Integrated Sensing and Communications: Towards Dual-functional Wireless Networks for 6G and Beyond," *IEEE J. Sel. Areas Commun.*, vol. 40, no. 6, pp. 1728–1767, Jun. 2022.
- [5] A. Kaushik, E. Vlachos, J. Thompson, M. Nekovee, and F. Coutts, "Towards 6G: Spectrally Efficient Joint Radar and Communication with RF Selection, Interference and Hardware Impairments," *IET Signal Process.*, vol. 16, no. 7, pp. 851–863, Sep. 2022.
- [6] A. Liu et al., "A Survey on Fundamental Limits of Integrated Sensing and Communication," *IEEE Commun. Surv. Tutor.*, vol. 24, no. 2, pp. 994–1034, Feb. 2022.
- [7] M. I. Skolnik, *Introduction to Radar Systems*, 2nd ed. McGraw-Hill, Inc., 1981.
- [8] Q. Yang, H. Zhang, and B. Wang, "Beamforming Design for Integrated Sensing and Wireless Power Transfer Systems," *IEEE Commun. Lett.*, vol. 27, no. 2, pp. 600–604, Feb. 2023.
- [9] P. Sun, H. Dai, and B. Wang, "Optimal Transmit Beamforming for Near-Field Integrated Sensing and Wireless Power Transfer Systems," *Intell. and Converged Netw.*, vol. 3, no. 4, pp. 378–386, Dec. 2022.
- [10] X. Li, X. Yi, Z. Zhou, K. Han, Z. Han, and Y. Gong, "Multi-User Beamforming Design for Integrating Sensing, Communications, and Power Transfer," in *Proc. IEEE WCNC*, 2023, pp. 1–6.
- [11] Y. Chen, H. Haocheng, J. Xu, and D. W. K. Ng, "ISAC Meets SWIPT: Multi-functional Wireless Systems Integrating Sensing, Communication, and Powering," *arXiv preprint arXiv:2211.10605v2*, 2023.
- [12] O. Rezaei, M. M. Naghsh, S. M. Karbasi, and M. M. Navebi, "Multi-UAV Enabled Integrated Sensing and Wireless Powered Communication: A Robust Multi-Objective Approach," *arXiv preprint arXiv:2307.14299v1*, 2023.
- [13] J. Kim, B. Clerckx, and P. D. Mitcheson, "Signal and System Design for Wireless Power Transfer: Prototype, Experiment and Validation," *IEEE Trans. Wirel. Commun.*, vol. 19, no. 11, pp. 7453–7469, Nov. 2020.
- [14] R. Morsi, V. Jamali, A. Hagelauer, D. W. K. Ng, and R. Schober, "Conditional Capacity and Transmit Signal Design for SWIPT Systems With Multiple Nonlinear Energy Harvesting Receivers," *IEEE Trans. Commun.*, vol. 68, no. 1, pp. 582–601, Jan. 2020.
- [15] N. Shanin, L. Cottatellucci, and R. Schober, "Optimal Transmit Strategy for Multi-User MIMO WPT Systems With Non-Linear Energy Harvesters," *IEEE Trans. Commun.*, vol. 70, no. 3, pp. 1726–1741, Mar. 2022.
- [16] B. Clerckx, "Wireless Information and Power Transfer: Nonlinearity, Waveform Design, and Rate-Energy Tradeoff," *IEEE Trans. Signal Process.*, vol. 66, no. 4, pp. 847–862, Feb. 2018.
- [17] Y. Sun, P. Babu, and D. P. Palomar, "Majorization-Minimization Algorithms in Signal Processing, Communications, and Machine Learning," *IEEE Trans. Signal Process.*, vol. 65, no. 3, pp. 794–816, Feb. 2017.
- [18] S. Diamond and S. Boyd, "CVXPY: A Python-Embedded Modeling Language for Convex Optimization," *J. Mach. Learn. Res.*, vol. 17, no. 83, pp. 1–5, 2016.
- [19] G. Lanckriet and B. K. Sriperumbudur, "On the Convergence of the Concave-Convex Procedure," *Adv. in Neural Inf. Process. Syst.*, vol. 22, pp. 1759–1767, Dec. 2009.
- [20] R. Zhang and C. K. Ho, "MIMO Broadcasting for Simultaneous Wireless Information and Power Transfer," *IEEE Trans. Wirel. Commun.*, vol. 12, no. 5, pp. 1989–2001, May 2013.
- [21] S. P. Boyd and L. Vandenberghe, *Convex Optimization*. Cambridge University Press, 2004.